Self-reconstructing spatiotemporal light bullets

I. Gražulevičiūtė,[1] G. Tamošauskas,[1] V. Jukna,[2] A. Couairon,[2] D. Faccio,[3] and A. Dubietis,[1,*]

[1]*Department of Quantum Electronics, Vilnius University, Saulėtekio Ave. 9, Building 3, LT-10222 Vilnius, Lithuania*
[2]*Centre de Physique Théorique, CNRS, Ecole Polytechnique, F-91128 Palaiseau, France*
[3]*School of Engineering & Physical Sciences, Heriot-Watt University, Edinburgh EH14-4AS, United Kingdom*
[*]*audrius.dubietis@ff.vu.lt*

Abstract: We show that spatiotemporal light bullets generated by self-focusing and filamentation of 100 fs, 1.8 μm pulses in a dielectric medium with anomalous group velocity dispersion (sapphire) are extremely robust to external perturbations. We present the experimental results supported by the numerical simulations that demonstrate complete spatiotemporal self-reconstruction of the light bullet after hitting an obstacle, which blocks its intense core carrying the self-compressed pulse, in nonlinear as well as in linear (free-space) propagation regimes.

OCIS codes: (190.5940) Self-action effects; (260.5950) Self-focusing; (320.5520) Pulse compression; (320.7110) Ultrafast nonlinear optics.

References and links

1. A. Couairon and A. Mysyrowicz, "Femtosecond filamentation in transparent media," Phys. Rep. **441,** 47–189 (2007).
2. A. Dubietis, E. Gaižauskas, G. Tamošauskas, and P. Di Trapani, "Light filaments without self-channeling," Phys. Rev. Lett. **92,** 253903 (2004).
3. M. A. Porras, A. Parola, D. Faccio, A. Dubietis, and P. Di Trapani,"Nonlinear unbalanced Bessel beams: stationary conical waves supported by nonlinear losses," Phys. Rev. Lett. **93,** 153902 (2004).
4. A. Lotti, A. Couairon, D. Faccio, and P. Di Trapani, "Energy-flux characterization of conical and space-time coupled wave packets," Phys. Rev. A **81,** 023810 (2010).
5. F. Courvoisier, V. Boutou, J. Kasparian, E. Salmon, G. Mejèan, J. Yu, and. J. P. Wolf, "Light filaments transmitted through clouds," Appl. Phys. Lett. **83,** 213–215 (2003).
6. M. Kolesik and J.V. Moloney, "Self-healing femtosecond light filaments," Opt. Lett. **29,** 590–592 (2004).
7. A. Dubietis, E. Kučinskas, G. Tamošauskas, E. Gaižauskas, M. A. Porras, and P. Di Trapani, "Self-reconstruction of light filaments," Opt. Lett. **29,** 2893–2895 (2004).
8. W. Liu, F. Théberge, E. Arévalo, J.-F. Gravel, A. Becker, and S. L. Chin, "Experiment and simulations on the energy reservoir effect in femtosecond light filaments," Opt. Lett. **30,** 2602–2604 (2005).
9. S. Eisenmann, J. Peñano, P. Sprangle, and A. Zigler, "Effect of an energy reservoir on the atmospheric propagation of laser-plasma filaments," Phys. Rev. Lett. **100,** 155003 (2008).
10. S. Skupin, L. Bergé, U. Peschel, and F. Lederer, "Interaction of femtosecond light filaments with obscurants in aerosols," Phys. Rev. Lett. **93,** 023901 (2004).
11. G. Méchain, G. Méjean, R. Ackermann, P. Rohwetter, Y.-B. André, J. Kasparian, B. Prade, K. Stelmaszczyk, J. Yu, E. Salmon, W. Winn, L. A. Schlie, A. Mysyrowicz, R. Sauerbrey, L. Wöste, and J.-P. Wolf, "Propagation of fs TW laser filaments in adverse atmospheric conditions," Appl. Phys. B **80,** 785–789 (2005).
12. G. Méjean, J. Kasparian, J. Yu, E. Salmon, S. Frey, J.-P. Wolf, S. Skupin, A. Vinçotte, R. Nuter, S. Champeaux, and L. Bergé, "Multifilamentation transmission through fog," Phys. Rev. E **72,** 026611 (2005).
13. A. Houard, M. Franco, B. Prade, A. Durécu, L. Lombard, P. Bourdon, O. Vasseur, B. Fleury, C. Robert, V. Michau, A. Couairon, and A. Mysyrowicz, "Femtosecond filamentation in turbulent air," Phys. Rev. A **78,** 033804 (2008).

14. V. Jukna, G. Tamošauskas, G. Valiulis, M. Aputis, M. Puida, F. Ivanauskas, and A. Dubietis, "Filamentation of ultrashort light pulses in a liquid scattering medium," Appl. Phys. B **94,** 175–179 (2009).
15. L. Bergé, S. Skupin, and G. Steinmeyer, "Temporal self-restoration of compressed optical filaments," Phys. Rev. Lett. **101,** 213901 (2008).
16. M. Mlejnek, E. M. Wright, and J. V. Moloney, "Dynamic spatial replenishment of femtosecond pulses propagating in air," Opt. Lett. **23,** 382–384 (1998).
17. A. Jarnac, G. Tamošauskas, D. Majus, A. Houard, A. Mysyrowicz, A. Couairon, and A. Dubietis, "Whole life cycle of femtosecond ultraviolet filaments in water," Phys. Rev. A **89,** 033809 (2014).
18. M. Kolesik, E. M. Wright, and J. V. Moloney, "Dynamic nonlinear X waves for femtosecond pulse propagation in water," Phys. Rev. Lett. **92,** 253901 (2004).
19. D. Faccio, M. A. Porras, A. Dubietis, F. Bragheri, A. Couairon, and P. Di Trapani, "Conical emission, pulse splitting, and X-wave parametric amplification in nonlinear dynamics of ultrashort light pulses," Phys. Rev. Lett. **96,** 193901 (2006).
20. D. Faccio, A. Averchi, A. Lotti, P. Di Trapani, A. Couairon, D. Papazoglou, and S. Tzortzakis, "Ultrashort laser pulse filamentation from spontaneous X Wave formation in air," Opt. Express **16,** 1565–1570 (2008).
21. D. McGloin and K. Dholakia, "Bessel beams: diffraction in a new light," Contemp. Phys. **46,** 15–28 (2005).
22. J. Broky, G. A. Siviloglou, A. Dogariu, and D. N. Christodoulides, "Self-healing properties of optical Airy beams," Opt. Express **16,** 12880–12891 (2008).
23. K. B. Chung, "Self-reconstruction of obstructed Bessel-X pulses modeled by the FDTD method," Opt. Commun. **320,** 43–48 (2014).
24. F. Silva, D. R. Austin, A. Thai, M. Baudisch, M. Hemmer, D. Faccio, A. Couairon, and J. Biegert, "Multi-octave supercontinuum generation from mid-infrared filamentation in a bulk crystal," Nature Commun. **3,** 807 (2012).
25. M. Hemmer, M. Baudisch, A. Thai, A. Couairon, and J. Biegert, "Self-compression to sub-3-cycle duration of mid-infrared optical pulses in dielectrics," Opt. Express **21,** 28095–28102 (2013).
26. M. Durand, A. Jarnac, A. Houard, Y. Liu, S. Grabielle, N. Forget, A. Durécu, A. Couairon, and A. Mysyrowicz, "Self-guided propagation of ultrashort laser pulses in the anomalous dispersion region of transparent solids: a new regime of filamentation," Phys. Rev. Lett. **110,** 115003 (2013).
27. E. O. Smetanina, V. O. Kompanets, A. E. Dormidonov, S. V. Chekalin, and V. P. Kandidov, "Light bullets from near-IR filament in fused silica," Laser Phys. Lett. **10,** 105401 (2013).
28. D. Majus, G. Tamošauskas, I. Gražulevičiūtė, N. Garejev, A. Lotti, A. Couairon, D. Faccio, and A. Dubietis, "Nature of spatiotemporal light bullets in bulk Kerr media," Phys. Rev. Lett. **112,** 193901 (2014).
29. M. A. Porras, "A dissipative attractor in the spatiotemporal collapse of ultrashort light pulses," Opt. Express **18,** 7376–7383 (2010).
30. M. A. Porras and F. Redondo, "On the stabilizing effect of nonlinear energy losses in light bullet propagation," J. Opt. Soc. Am. B **30,** 603–609 (2013).
31. M. A. Porras, "Nonlinear light bullets in purely lossy, self-focusing media," Appl. Phys. B **103,** 591–596 (2011).
32. M. A. C. Potenza, S. Minardi, J. Trull, G. Blasi, D. Salerno, A. Varanavičius, A. Piskarskas, and P. Di Trapani, "Three dimensional imaging of short pulses," Opt. Commun. **229**, 381–390 (2004).
33. A. Couairon, E. Brambilla, T. Corti, D. Majus, O. de J. Ramirez-Gongora, and M. Kolesik, "Practitioner's guide to laser pulse propagation models and simulation," Eur. Phys. J. Special Topics **199.** 5–76 (2011).
34. M. J. Weber, *Handbook of Optical Materials* (CRC, 2003).
35. L. V. Keldysh, "Ionization in the field of a strong electromagnetic wave," Sov. Phys. JETP **20,** 1307–1314 (1965).
36. M. Durand, K. Lim, V. Jukna, E. McKee, M. Baudelet, A. Houard, M. Richardson, A. Mysyrowicz and A. Couairon, "Blueshifted continuum peaks from filamentation in the anomalous dispersion regime," Phys. Rev. A **87,** 043820 (2013).
37. E. Gaižauskas, A. Dubietis, V. Kudriašov, V. Sirutkaitis, A. Couairon, D. Faccio, and P. Di Trapani, "On the role of conical waves in self-focusing and filamentation of femtosecond pulses with nonlinear losses," Top. Appl. Phys. **114,** 457–479 (2009).

1. Introduction

Filamentation of intense femtosecond laser pulses in transparent dielectric media exhibit universal features, such as long range propagation, which produces a narrow plasma channel, self-cleaning and robustness of the spatial mode, complex temporal dynamics, such as shock front generation, pulse splitting and compression, and supercontinuum generation accompanied by colored conical emission [1]. Light filament is a dynamic structure that consists of a narrow high-intensity central core surrounded by an extended low intensity periphery, often termed energy reservoir, which carries a major portion of the energy. Strong coupling between the core and periphery arises from the interplay between nonlinear losses (multiphoton absorption and

ionization), self-focusing and diffraction, resulting in reshaping of the Gaussian input beam into a Bessel-like beam [2, 3]; the sub-diffractive propagation of the central core, which carries an ultrashort pulse, is structurally sustained by the conical energy flux from the periphery [4].

The most obvious manifestation of mutual coupling between the core and periphery is highlighted by experiments and simulations, which demonstrate how the central core after being completely blocked, is able to self-reconstruct very shortly after the obstacle [2, 5–7]. And on the contrary, if a filament passes through a pinhole which transmits only a narrow core and blocks the periphery, the filamentary propagation is terminated, the transmitted central core quickly diffracts and decays, as verified under various operating conditions [2, 8, 9].

Self-reconstruction property allows light filaments to be transmitted without an apparent change of the spatial profile through strongly turbulent and scattering media, such as atmospheric haze, fog, rain and clouds, as demonstrated by numerical simulations and by field and laboratory experiments [5, 6, 10–14], holding a great potential for various atmospheric, technological and biomedical applications. Numerical simulations also suggest that light filaments carrying few-optical cycle pulses are able to reconstruct their temporal structure when propagating in the medium with huge discontinuity of nonlinear properties, such as gas-glass-gas interface [15]. The reconstruction property lies on the basis of dynamical spatial replenishment [16] and interpretation of recurrent focusing and defocusing cycles associated with pulse splitting and replenishment events in the time domain [17]. Exceptional robustness of femtosecond filaments arises from their Bessel-like spatial profile [2, 3] and, more-generally, from the X-shaped spatiotemporal intensity distribution, which is universal for all the media with normal group velocity dispersion (GVD), see e.g. [18–20]. It is worth mentioning that self-healing (self-reconstruction) is an intrinsic property of linear conical waves, e.g. Bessel [21] and Airy [22] beams and Bessel X-waves [23] owing to their transverse energy flux.

Propagation of intense femtosecond laser pulses in transparent dielectrics with anomalous GVD leads to a new filamentation regime, in which self-focusing of the beam is concurrent with the pulse compression in time due to the interplay between self-phase modulation and anomalous GVD. In this regime, self-compression of the pulses down to few optical cycles could be achieved [24, 25], eventually giving rise to formation of spatiotemporal light bullets – self-compressed nonlinear objects, that thereafter exhibit quasistationary propagation over distances exceeding many diffraction and dispersion lengths [26], or recurrent self-compression cycles at higher input energy [27]. More recently, high dynamic range measurements of spatiotemporal intensity profiles, corresponding energy fluxes and sub-diffractive and dispersive propagation in free space disclosed that spatiotemporal light bullets bear the basic properties of polychromatic Bessel-like beams that clearly distinguishes them from soliton-like objects [28]. It was also demonstrated theoretically that the nonlinear losses (multiphoton absorption and ionization) experienced by an intense central core play a stabilizing role on the overall bullet propagation dynamics [29, 30], suggesting a potential robustness of the light bullets to external perturbations as well [31].

In this paper we experimentally and numerically demonstrate that spatiotemporal light bullets generated by filamentation of femtosecond laser pulses in media with anomalous GVD, exhibit a property of full spatiotemporal reconstruction. In particular, we show that the narrow central core of the bullet, which carries the self-compressed pulse, after being blocked by the beam stopper, fully restores its spatial and temporal dimensions. Moreover, we find that owing to conical nature, the light bullet self-reconstructs in free-space as well, and thereafter propagates in sub-diffractive and dispersive manner, as in unperturbed case.

2. Experimental setup

A sketch of the experimental setup is depicted in Fig. 1. The experiment was performed using 100 fs, 1.8 μm idler pulses from a commercial optical parametric amplifier (Topas-C, Light Conversion Ltd.), OPA, which was pumped by a fraction of fundamental harmonics of the amplified Ti:sapphire laser system (Spitfire-PRO, Newport-Spectra Physics). The OPA output beam was suitably attenuated by a variable attenuator AT consisting of two Glan prisms for precise input energy control, spatially filtered and focused by an $f = +100$ mm lens L1 into 60-μm FWHM spot size located at the front face of sapphire crystal, which possesses anomalous GVD for the input wavelength.

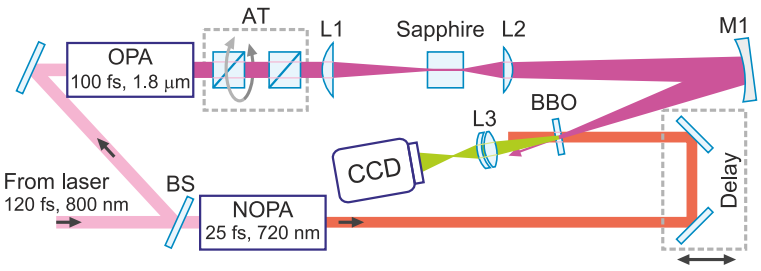

Fig. 1. Experimental setup. OPA, optical parametric amplifier; NOPA, noncollinear optical parametric amplifier; BS, beam splitter; AT, variable attenuator for energy control; L1, L2, L3, lenses; M1, concave mirror; BBO, thin beta-barium borate crystal for broadband sum-frequency generation.

The spatiotemporal intensity distribution of the light bullet was measured by three-dimensional imaging technique, based on recording spatially-resolved cross-correlation function, see e.g. [28, 32] for the details. For that purpose, the emerging light bullet (at the output face of the nonlinear medium) was imaged (with 5$\times$ magnification) by a lens L2 and concave mirror M1 onto a 20-μm-thick beta-barium borate crystal (BBO) and gated by means of broadband sum-frequency generation with a short, 25-fs pulse with central wavelength of 720 nm from a noncollinear optical parametric amplifier (Topas-White, Light Conversion Ltd.), NOPA, which was pumped by the second harmonic pulses of the Ti:sapphire laser system. The small crystal thickness guaranteed broadband phase matching in the small-signal conversion regime. The cross-correlation signal with a central wavelength of 515 nm was imaged by a lens L3 onto the CCD camera (Grasshopper 2, Point Grey) with a pixel size of 4.4 μm and 14-bit digitalization. The spatiotemporal intensity (x,y,t) distribution of the light bullet was reconstructed from a series of cross-correlation images recorded by changing the time delay of the gating pulse in a 8-fs step. The entire evolution of the spatiotemporal intensity distribution (in the following referred as spatiotemporal cross-correlation function) of the light bullet versus propagation distance z was captured by placing sapphire samples of different lengths, keeping the output face of the sample at the same fixed position (as necessary for imaging), and translating the position of the focusing lens L1 accordingly, to ensure the location of the input focal plane at the front face of the sample. The propagation of the light bullet in free space (air) was measured by simply shifting the image plane outside the sapphire crystal.

3. Experimental results

In the first experiment, formation and propagation dynamics of an unperturbed light bullet was captured in full four-dimensional (x,y,t,z) space, using a set of sapphire samples with different lengths. With the input pulse energy of 3.25 μJ (which corresponds to 3.6 P_{cr}, where

$P_{cr} = 0.15\lambda^2/n_0 n_2 = 10$ MW is the critical power for self-focusing in sapphire, where λ is wavelength, n_0 and n_2 are linear and nonlinear refractive indexes, respectively), the light bullet composed of a narrow intense central core of 18 μm FWHM diameter, which carries the self-compressed pulse of 38 fs duration, surrounded by an extended ring-shaped spatiotemporal periphery, emerged after the nonlinear focus at $z \approx 6$ mm of propagation. Figure 2 shows the examples of the spatiotemporal cross-correlation functions of the input Gaussian pulsed beam and the light bullet recorded at $z = 9$ mm and $z = 15$ mm of propagation. Despite somewhat different input conditions, the recorded spatial and temporal dimensions of the light bullet were essentially identical to the previously reported ones [28].

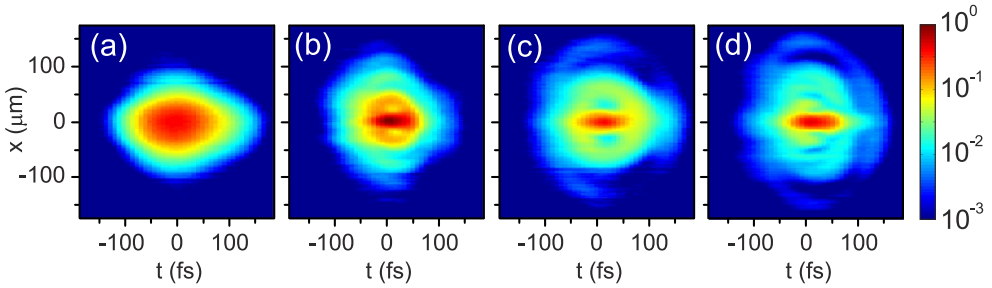

Fig. 2. Measured spatiotemporal cross-correlation functions of (a) the input Gaussian wave packet and the light bullet at the output face of (b) $z = 9$ mm and (c) $z = 15$ mm long sapphire samples. (d) shows the spatiotemporal cross-correlation function of the light bullet, which was formed after $z = 9$ mm propagation in the first sapphire sample, passed the 0.8 mm air gap and propagated another 6 mm in the second sapphire sample. Note the logarithmic intensity scale.

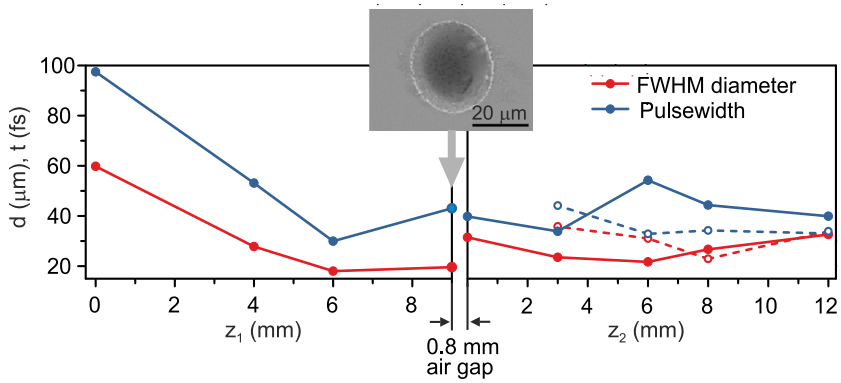

Fig. 3. FWHM diameter and pulsewidth of the central core as functions of propagation distance: solid curves – unperturbed light bullet, dashed curves – self-reconstructed light bullet. z_1 and z_2 denote the propagation lengths in the first and in the second sapphire sample, respectively. Inset shows an electronic microscope image of the beam stopper that blocked the central core at the output of the first sapphire crystal.

Thereafter, the measurements were repeated using a combined medium consisting of two sapphire samples separated by 0.8 mm air gap. The length of the first sapphire sample was set fixed at $z_1 = 9$ mm, where the light bullet is completely formed, as shown in Fig. 2(b). After that, the light bullet passed the air gap and entered the second sapphire sample, whose length z_2

was varied between 3 and 12 mm. We found that the discontinuity of the properties (nonlinear-linear-nonlinear) of that combined medium, had only a minor effect on the bullet propagation: in the second sapphire crystal the light bullet preserves its spatiotemporal shape [Fig. 2(d)], which is almost undistinguishable from that recorded in the case of unperturbed propagation, as shown in Fig. 2(c). We also verified that the central core of the light bullet retains its spatial and temporal dimensions in the second sapphire crystal if the air gap is increased up to 2 mm (not shown). The experimental data is summarized by solid curves in Fig. 3, which plots the pulsewidth t and FWHM diameter d of the central core versus the propagation lengths in the first (z_1) and in the second (z_2) sapphire sample.

In the second experiment we demonstrate how the light bullet is able to self-reconstruct and completely recover its self-compressed central core after being blocked by a beam stopper. An opaque sharp-edged damage crater of 25 μm diameter (see the inset of Fig. 3), produced by laser micromachining on the output face of the first sapphire crystal served as a beam stopper. The crystal was mounted on a two-dimensional translation stage, which allowed fine adjustment of the beam stopper position with respect to the laser beam so as to exactly block the central core of the light bullet. Figure 4 illustrates the self-reconstruction dynamics in detail by presenting the spatiotemporal cross-correlation functions of the light bullet at various stages of propagation: at the output face of the first sapphire sample, where the central core was blocked by the beam stopper, at the input face of the second sapphire sample (after passing the air gap) and at several propagation lengths in the second sapphire sample.

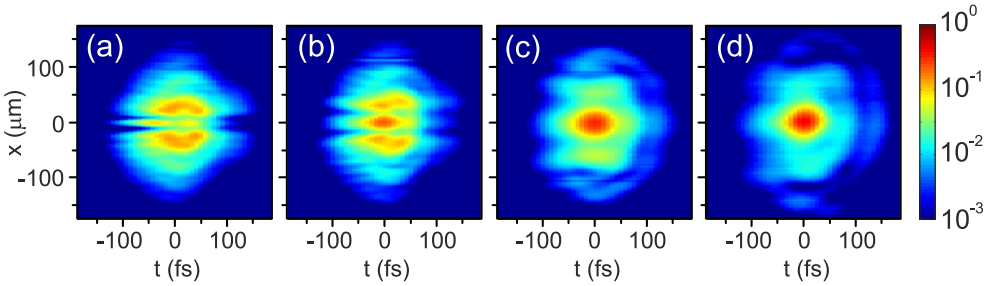

Fig. 4. Self-reconstruction of the light bullet. The spatiotemporal cross-correlation functions: (a) at the output face of the first sapphire sample ($z_1 = 9$ mm), (b) at the input face of the second sapphire sample ($z_2 = 0$ mm), and after propagation of (c) $z_2 = 3$ mm and (d) $z_2 = 6$ mm in the second sapphire sample.

We observe that the central core of the light bullet is rebuilt just after 3 mm of propagation in the second sapphire crystal (that is the length of the shortest available sample) and thereafter shrinks to original spatial and temporal dimensions with further propagation (for $z_2 > 8$ mm), as summarized by dashed curves in Fig. 3. Interestingly, the self-reconstruction of the central core already becomes detectable after passing the 0.8 mm air gap between the two sapphire samples, as seen from Fig. 4(b). Indeed, linear contribution due to the conical nature of the beam to its spatial self-reconstruction was highlighted in the case of light filaments in water [7].

In order to investigate this effect in more detail, in the entire space-time domain, we removed the second sapphire sample and monitored free space propagation of the light bullet. First of all, we recorded the evolution of the spatiotemporal cross-correlation functions of unperturbed light bullet, as it exits the first sapphire crystal of 9 mm length and propagates in air. Owing to strong spatiotemporal coupling, which establishes after the nonlinear focus, in free space propagation the light bullet experiences dispersive broadening along with reduced diffractive spreading of the central core (as compared to the Gaussian beam of identical diameter), as

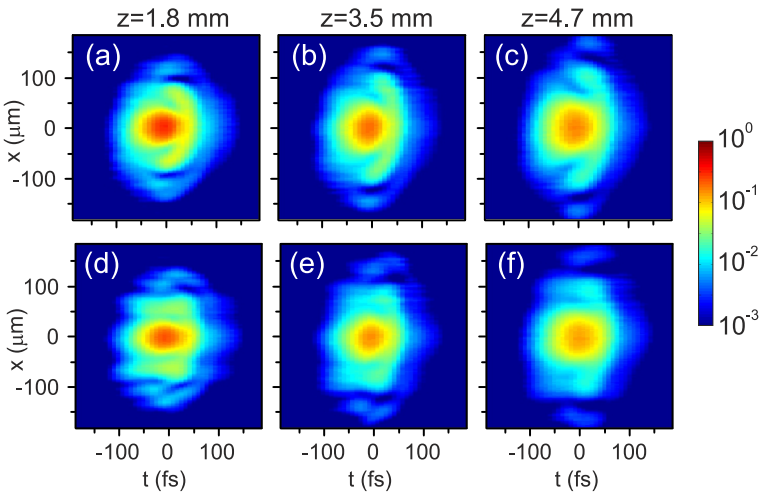

Fig. 5. Free space propagation of unperturbed (top-row) and self-reconstructed (bottom row) light bullet. z denotes the propagation distance in air.

shown in Figs. 5(a)–5(c), in line with the results of the previous study [28]. Figures 5(d)–5(f) show free space propagation of the blocked light bullet, which reconstructs its central core after 1.8 mm propagation in air, as illustrated in Fig. 5(d) and thereafter continues propagation exactly in the same manner (dispersive and sub-diffractive) and with almost undistinguishable spatiotemporal shape as the unperturbed light bullet, as illustrated in Figs. 5(e) and 5(f).

4. Numerical model

Ultrashort pulse filamentation in the anomalous GVD regime was numerically simulated by the unidirectional nonparaxial propagation equation for the spectral components of the laser pulse envelope $\hat{E}(\omega,k_\perp,z)$ [33]:

$$\frac{\partial \hat{E}}{\partial z} = i\left(\sqrt{k^2(\omega)-k_\perp^2}-k_0-k_0'\omega\right)\hat{E}+i\frac{\omega}{2n(\omega)c}\varepsilon_0^{-1}\left(\hat{P}+i\frac{\hat{J}}{\omega}\right), \tag{1}$$

where $k(\omega)$ denotes the dispersion relation in the medium, $k_\perp$ is the transverse wave vector, $n(\omega)$ is the refractive index of the medium calculated from a Sellmeier equation [34], from which $k_0 \equiv k(\omega_0)$ and $k_0' \equiv dk/d\omega|_{\omega_0}$ were evaluated at the central laser frequency.

The nonlinear polarization and current source terms $P(t,r,z)$ and $J(t,r,z)$ were computed in the space-time domain, assuming revolution symmetry:

$$\varepsilon_0^{-1}P = 2n_0n_2|E|^2E, \tag{2}$$

$$\varepsilon_0^{-1}J = n_0c\left[\sigma(1+i\omega_0\tau_c)\rho+\frac{WU_g}{|E|^2}\left(1-\frac{\rho}{\rho_{nt}}\right)\right]E, \tag{3}$$

where n_0 and n_2 are the linear and nonlinear refractive indexes, respectively, σ is the cross section for inverse Bremsstrahlung, τ_c is the effective collision time, ρ is the density of electrons generated during propagation, ρ_{nt} is the density of neutral molecules, W is the rate of optical field ionization calculated from Keldysh's theory [35] with electron-hole mass ratio $m^*=1$, and U_g is the band gap. The density of electrons in the conduction band was obtained by a simple rate equation in the form:

$$\frac{\partial \rho}{\partial t} = W(\rho_{nt} - \rho) + \frac{\sigma}{U_g}|E|^2\rho(1 - \frac{\rho}{\rho_{nt}}) - \frac{\rho}{\tau_{rec}}, \quad (4)$$

where the terms on the right hand side describe photoionization, ionization by avalanche and recombination, respectively, where τ_{rec} is the free electron recombination time.

Table 1. Input beam and material parameters used in the numerical simulation.

Parameter	Value	Parameter	Value
λ	1800 nm	U_g	8.7 eV
t_p	100 fs	ρ_{nt}	2.1×10^{22} cm^{-3}
w_0	60 μm	τ_c	1 fs
n_0	1.74	m^*	1
n_2	1.8×10^{-16} cm^2/W	τ_{rec}	150 fs

The numerical simulations were performed with $w_0 = 60$ μm FWHM input beam size and $t_p = 100$ fs input pulse FWHM width with the spectral width corresponding to a 60 fs pulse, as verified from experimental input pulse characterization, and which was accounted by setting an initial positive linear chirp. The relevant parameters of the input pulse and the nonlinear medium used in the simulation are provided in Table 1.

5. Simulation results

Figure 6 presents a summary of the numerical simulations. The spatiotemporal profile of the whole wave packet, as shown in Fig. 6(a) reveals two distinct spatiotemporal structures: an O-shaped intensity distribution with a narrow spatiotemporal intensity peak located at the pulse center, which is associated with elliptical far-field spectrum [28,36] and much weaker, V-shaped intensity distribution at the pulse tail, corresponding to the blue peak in the visible part of supercontinuum emission [36]. These two distinct spectral features are separated by a frequency gap, and in the space-time domain refer to the light bullet and dispersive wave, respectively. Figure 6(e) shows the spatiotemporal intensity profile of the light bullet only, that is produced by reducing the spectral (to 400 nm around the pump wavelength) and angular (to $\pm$6 deg from the beam axis) extent, as corresponding to experimentally converted spectral bandwidth and acceptance angle of BBO crystal in the cross-correlation measurements. Notice that such filtering removes the temporal features (i.e. the dispersive wave and steep shock fronts) associated with the visible and near infrared part of the spectrum, as well as results in an increase of the diameter and pulsewidth of the central core due to loss of marginal spectral and angular components contributing to the light bullet itself.

In simulating self-reconstruction, a super-Gaussian obstacle with the diameter of 8 μm, which produced the same amount (14%) of experimentally measured energy losses was used; the resulting spatiotemporal profiles are shown in Figs. 6(b) and 6(f). Numerical simulation revealed that even after such energy loss and subsequent propagation through the air gap, the light bullet self-reconstructs its central core, which carries the self-compressed pulse, as illustrated in Figs. 6(c) and 6(g). Figures 6(d) and 6(h) show the spatiotemporal profiles of the light bullet, which reconstructs its central core in free space propagation due to conical energy flux and Arago spot effect [37], and which thereafter, in the absence of nonlinearity, experiences sub-diffractive and dispersive spreading.

Figures 6(i)–6(l) show the corresponding numerically simulated cross-correlation functions of the spatiotemporal intensity profiles shown in Figs. 6(e)–6(h), as produced with 25 fs gating pulse. Note that the spatiotemporal intensity profiles look very similar to cross-correlation

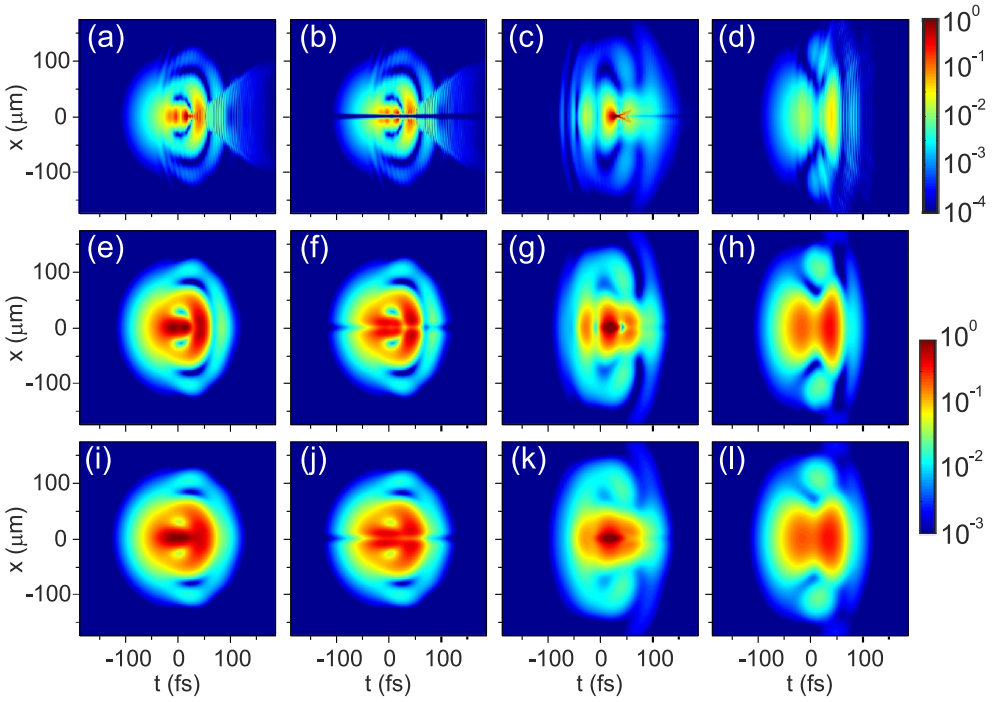

Fig. 6. Results of the numerical simulations. Top row – spatiotemporal intensity profiles of (a) light bullet at the output face of 9 mm long first sapphire sample, (b) blocked bullet, and self-reconstructed bullet after propagation (c) of 6 mm in a second sapphire sample, (d) of 3.5 mm in air. Middle row – spatiotemporal intensity profiles of the light bullet after reduction of spectral and angular extent (see text for details). Bottom row – corresponding cross-correlation functions generated with 25-fs gating pulse.

functions; just the finest features are lost in the latter due to limited temporal resolution set by the gating pulse. An excellent agreement between the results of numerical simulation and experiment is achieved, as highlighted by almost perfect coincidence of the numerically simulated and experimentally measured cross-correlation functions at various stages of the light bullet propagation.

6. Conclusions

In conclusion, our results demonstrate that spatiotemporal light bullets, generated by self-focusing and filamentation of femtosecond infrared laser pulses in solid-state dielectric medium with anomalous GVD, are remarkably robust objects, whose spatiotemporal robustness comes from conical energy flux, which establishes after the nonlinear focus. Firstly, we have shown that the light bullet is able to retain its narrow central core and short pulse duration after a linear stage of propagation (passing the air gap between two sapphire crystals), where it experiences dispersive broadening and sub-diffractive spreading. Secondly, we demonstrate that the light bullet completely self-reconstructs after hitting a beam stopper, which blocks its intense core carrying the self-compressed pulse. And thirdly, we demonstrate that the light bullet self-reconstructs its central core also in the absence of nonlinearity, in free space propagation; in this case however, the reconstructed central core experiences dispersive spreading, along with yet sub-diffractive propagation. A comparison of the self-reconstruction in the nonlinear medium

and in free space propagation highlights the importance of both, linear and nonlinear contributions to the self-reconstruction process. Our results also explicitly demonstrate the crucial role of the energy reservoir and provide yet another, to date the most straightforward proof of the conical nature of spatiotemporal light bullets generated by self-focusing and filamentation of femtosecond laser pulses in media with anomalous GVD.

Acknowledgment

This research was funded by the European Social Fund under the Global Grant measure, grant No. VP1-3.1-ŠMM-07-K-03-001.